

## Supplementary Information

### Blue light-induced low mechanical stability of Ruthenium-based coordination bonds: an AFM-based single-molecule force spectroscopy study

Mohd. Muddassir\*

Department of Chemistry, College of Science, King Saud University, Riyadh 11451,  
Saudi Arabia.

Corresponding Author Email: [mmohammadarshad@ksu.edu.sa](mailto:mmohammadarshad@ksu.edu.sa);  
muddassirchem@gmail.com

#### Table of Contents

Supporting Tables

**Table S1** Selected bond lengths (Å) and angles (°) for [(bpy)<sub>2</sub>Ru(4-pyNH<sub>2</sub>)<sub>2</sub>](PF<sub>6</sub>)<sub>2</sub>

**Table S2** Selected bond lengths (Å) and angles (°) for [(bpy)<sub>2</sub>Ru(4-pyNH<sub>2</sub>)<sub>2</sub>](PF<sub>6</sub>)<sub>2</sub>

Supporting Figures

**Figure S1** X-Ray Crystal structure of [(bpy)<sub>2</sub>Ru(4-pyNH<sub>2</sub>)<sub>2</sub>](PF<sub>6</sub>)<sub>2</sub>, thermal ellipsoids are drawn at 30% probability level. Remaining H-atoms, and counter ions have been omitted for clarity.

**Figure S2(A)** <sup>1</sup>HNMR spectrum of [(bpy)<sub>2</sub>Ru(4-pyNH<sub>2</sub>)<sub>2</sub>](PF<sub>6</sub>)<sub>2</sub> complex.

**Figure S2(B)** <sup>1</sup>HNMR spectrum of HA- Ru<sup>II</sup> complex. The ratio between Ru complex and sugar rings of the HA polymer is estimated ~22%.

**Figure S3(A)** IR spectrum of [(bpy)<sub>2</sub>Ru(4-pyNH<sub>2</sub>)<sub>2</sub>](PF<sub>6</sub>)<sub>2</sub> complex.

**Figure S3(B)** IR spectrum of HA- Ru<sup>II</sup> complex.

**Figure S4** UV-Vis spectrum of A) [(bpy)<sub>2</sub>Ru(4-pyNH<sub>2</sub>)<sub>2</sub>](PF<sub>6</sub>)<sub>2</sub> (in acetonitrile); B) HA- Ru<sup>II</sup> complex (in water).

**Figure S5** Emission spectrum of A)  $[(bpy)_2Ru(4-pyNH_2)_2](PF_6)_2$  (in acetonitrile); B) **HA- Ru<sup>II</sup>** complex (in water).

**Figure S6** Representative single-molecule force curves obtained from the control experiments. (a) No saw-tooth peaks were observed for the stretching of unmodified HA. (b) If no molecules were picked up, the approach and retrace traces typically overlap with each other.

**Figure S7** Representative single-molecule force curves obtained from the control experiments. HA-4-Iminopyridine. No saw-tooth peaks were observed. Red lines correspond to WLC fitting.

**Figure S8** The distributions of the persistence lengths of HA measured in the “multiple fishhooks” approach. A) Persistence lengths for force-extension traces obtained on **HA- Ru<sup>II</sup>** complex under normal condition (in black); B) Persistence lengths for force-extension traces obtained on **HA- Ru<sup>II</sup>** complex in continuous blue light illumination (in blue).

Table S1 Crystal structural data and refinement parameters for complexes [(bpy)<sub>2</sub>Ru(4-pyNH<sub>2</sub>)<sub>2</sub>](PF<sub>6</sub>)<sub>2</sub>

<b>1</b>	
CCDC No.	CCDC 1416079
Formula	C <sub>30</sub> H <sub>28</sub> N <sub>8</sub> Ru(PF <sub>6</sub> ) <sub>2</sub>
Formula weight	891.61
Temperature / K	293
Crystal system	Triclinic
Space group	<i>P</i> -1
<i>a</i> / Å	<u>10.768 (4)</u>
<i>b</i> / Å	<u>11.890 (4)</u>
<i>c</i> / Å	<u>16.120 (6)</u>
<i>α</i> / °	<u>104.401 (5)</u>
<i>β</i> / °	<u>98.576 (6)</u>
<i>γ</i> / °	<u>108.158 (5)</u>
Volume / Å <sup>3</sup>	<u>1841.1 (11)</u>
<i>Z</i>	2
<i>μ</i> / mm <sup>-1</sup>	0.61
<i>F</i> (000)	892
Crystal size / mm <sup>3</sup>	0.26×0.23×0.19
Index ranges	-12 ≤ <i>h</i> ≤ 12 -14 ≤ <i>k</i> ≤ 14 -19 ≤ <i>l</i> ≤ 19
Reflections collected	12100
Independent reflections	6290 [ <i>R</i> (int) = 0.092]
Data/restraints/parameters	6290/0/454
Goodness-of-fit on <i>F</i> <sup>2</sup>	1.23
Final <i>R</i> indexes [all data]	<i>R</i> <sub>1</sub> = 0.1384, <i>wR</i> <sub>2</sub> = 0.3835
Largest diff. peak/hole/e Å <sup>-3</sup>	1.75/-3.07

<sup>a</sup>  $R_1 = (\sum ||F_o| - |F_c||) / \sum |F_o|$ . <sup>b</sup>  $wR_2 = [\sum [w(F_o^2 - F_c^2)^2] / \sum [w(F_o^2)^2]]^{1/2}$ , where  $w = 1 / [\sigma^2(F_o^2) + (\alpha P)^2 + bP]$ .

Table S2 Selected bond lengths (Å) and angles (°) for **[(bpy)<sub>2</sub>Ru(4-pyNH<sub>2</sub>)<sub>2</sub>](PF<sub>6</sub>)<sub>2</sub>**

Ru1	N6		2.017(5)
Ru1	N1		2.042(4)
Ru1	N3		2.053(4)
Ru1	N7		2.054(4)
Ru1	N5		2.091(4)
Ru1	N2		2.108(4)
N6	Ru1	N1	77.94(17)
N6	Ru1	N3	96.84(17)
N1	Ru1	N3	171.81(17)
N6	Ru1	N7	88.27(16)
N1	Ru1	N7	94.64(15)
N3	Ru1	N7	78.78(16)
N6	Ru1	N5	175.81(16)
N1	Ru1	N5	98.23(17)
N3	Ru1	N5	86.78(17)
N7	Ru1	N5	90.36(15)
N6	Ru1	N2	89.84(16)
N1	Ru1	N2	87.61(15)
N3	Ru1	N2	98.77(16)
N7	Ru1	N2	176.70(16)
N5	Ru1	N2	91.71(15)

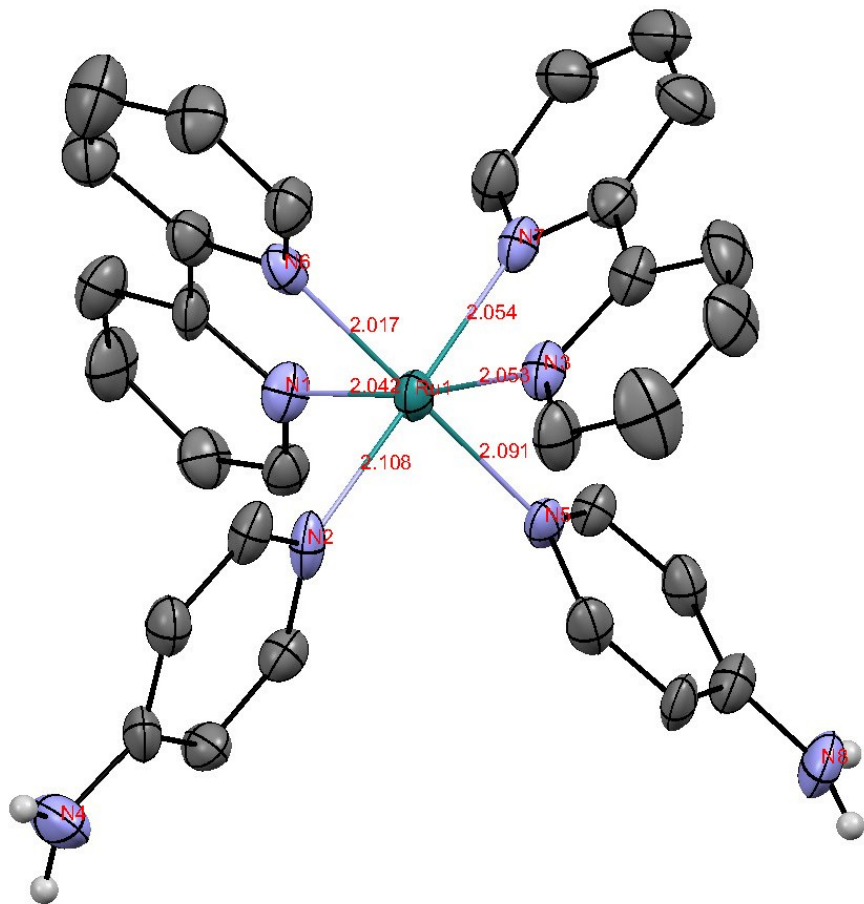


Figure S1

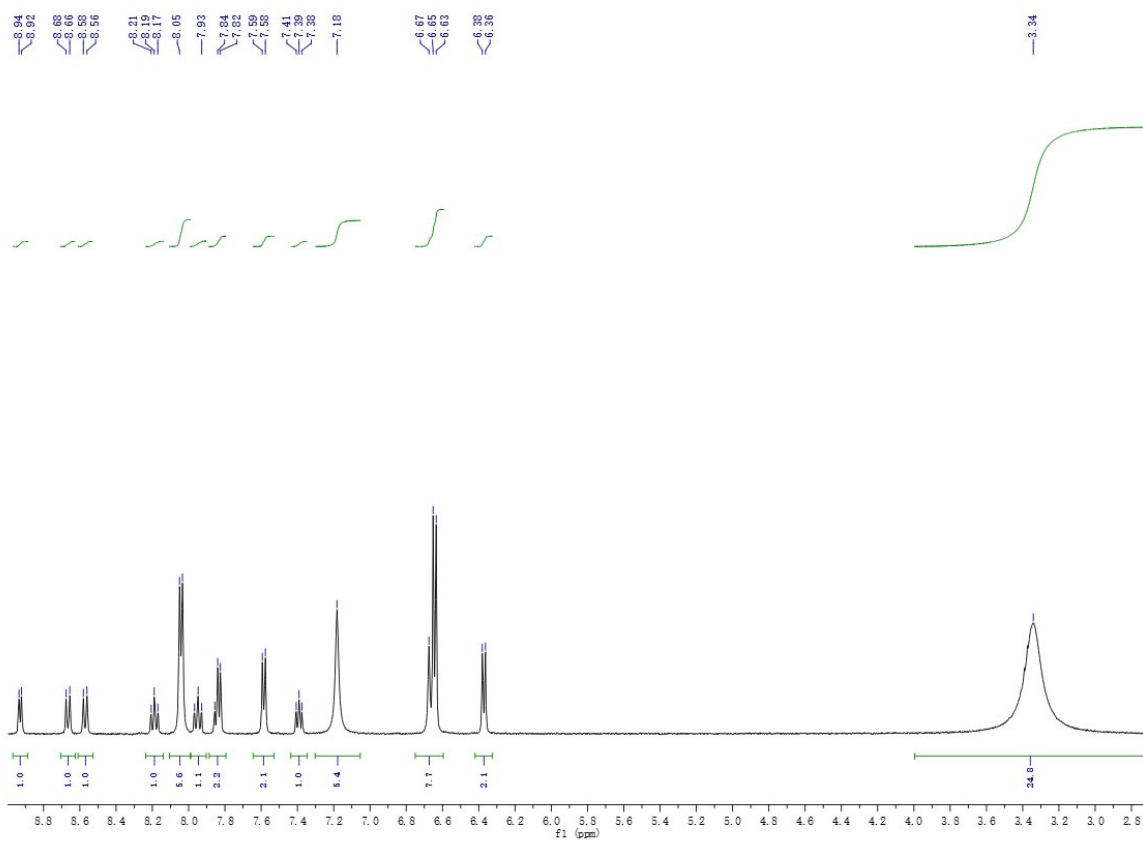


Figure S2(A)-.

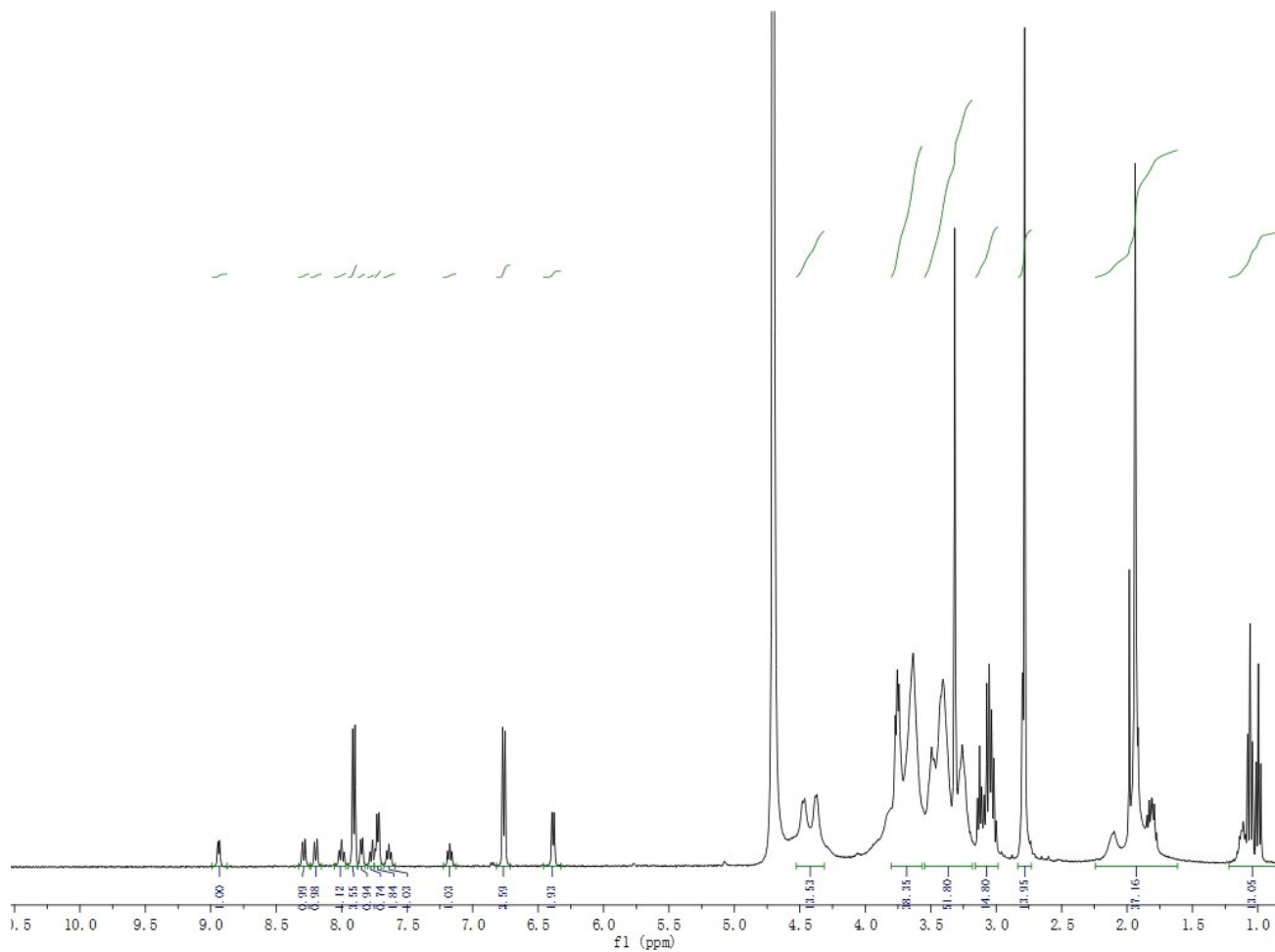


Figure S2(B)

Resonances at aromatic region (6.4-8.9ppm) verified the presence of Ru<sup>II</sup> complex, and their integrated ratios were compared with that of the N-acetyl glucosamine proton peak of native HA, appearing at ~1.9 ppm

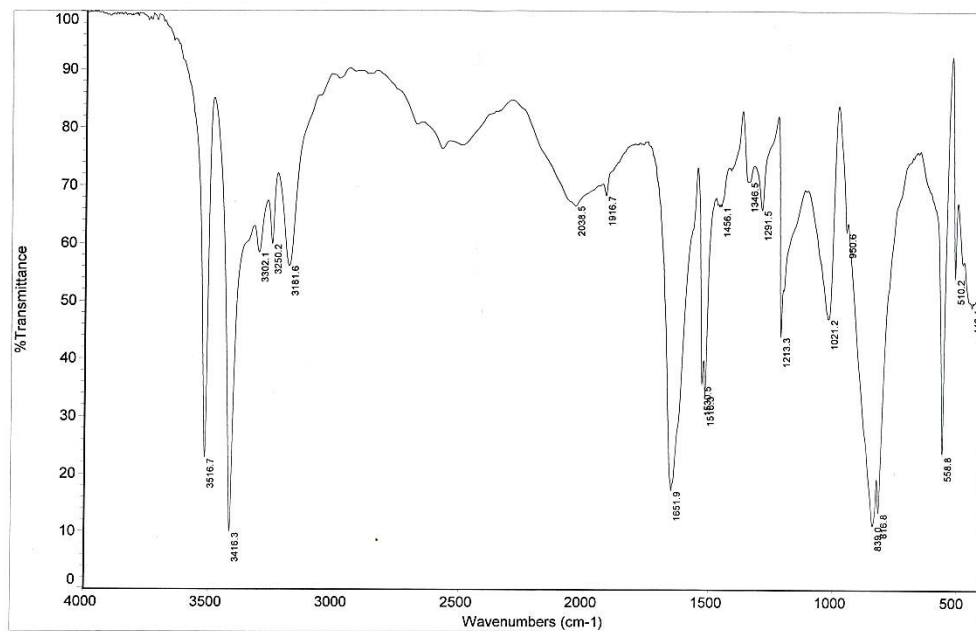


Figure S3(A)

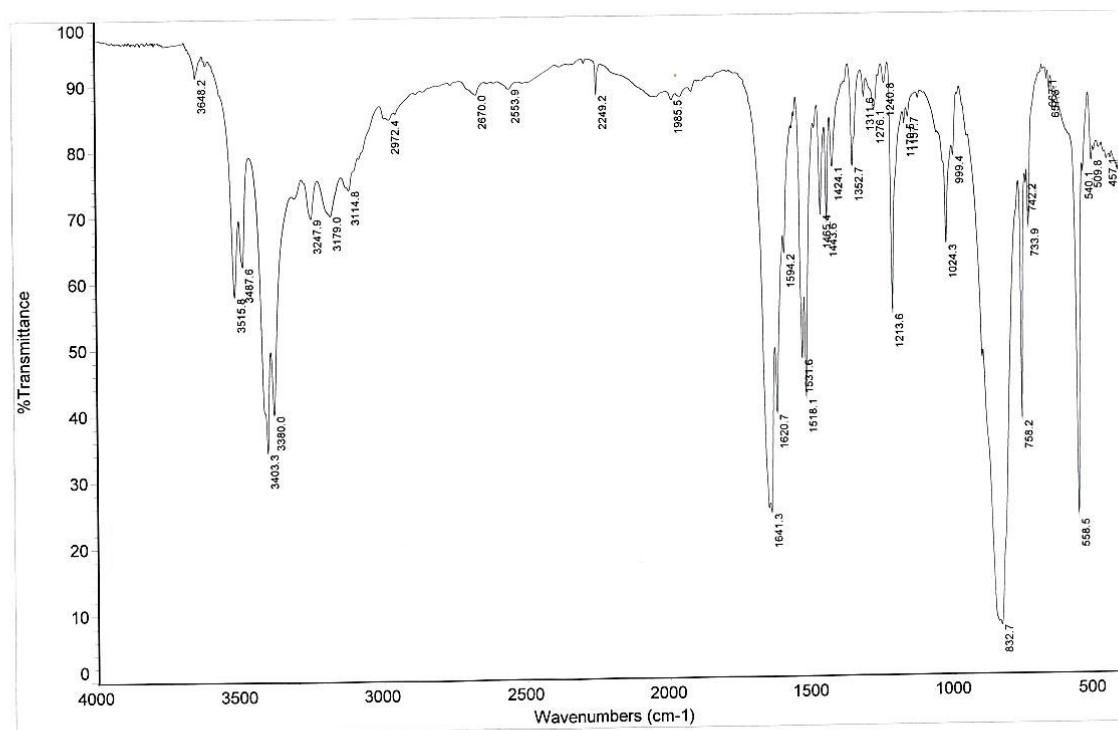
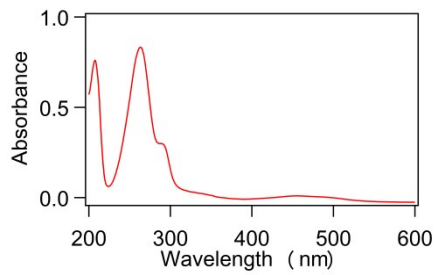
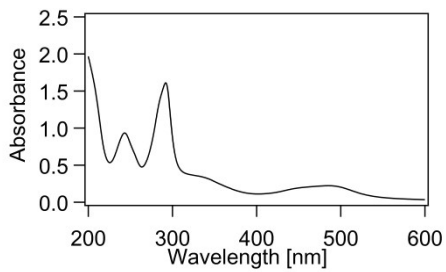


Figure S3(B)



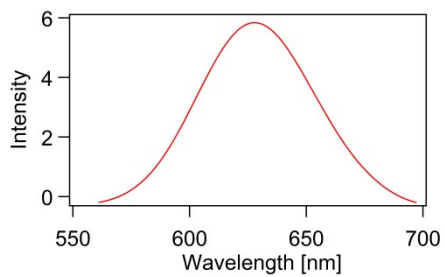


(A)

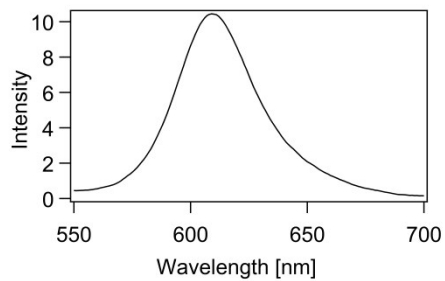


(B)

Figure S4



(A)



(B)

Figure S5

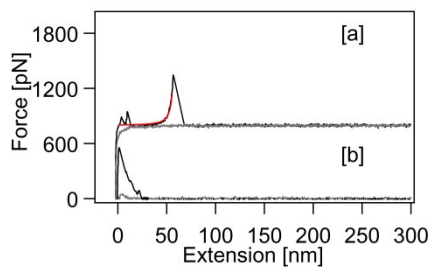


Figure S6

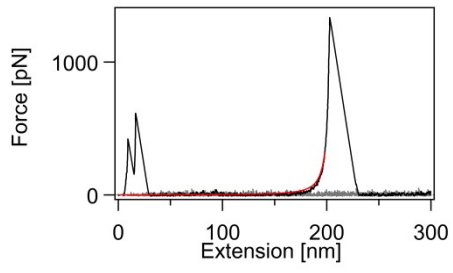
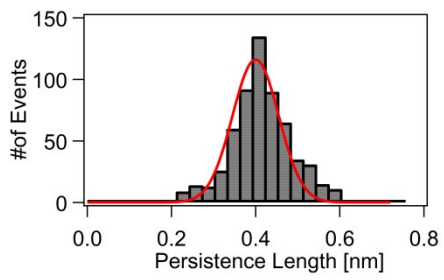
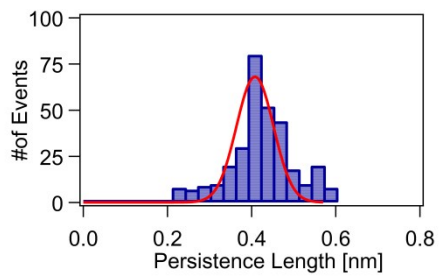


Figure S7



(A)



(B)

Figure S8